IOPscience iopscience.iop.org

Home Search Collections Journals About Contact us My IOPscience

Climate, not conflict, explains extreme Middle East dust storm

This content has been downloaded from IOPscience. Please scroll down to see the full text.

2016 Environ. Res. Lett. 11 114013

(http://iopscience.iop.org/1748-9326/11/11/114013)

View the table of contents for this issue, or go to the journal homepage for more

Download details:

IP Address: 155.41.125.132
This content was downloaded on 08/11/2016 at 15:04

Please note that terms and conditions apply.

Environmental Research Letters

LETTER

Climate, not conflict, explains extreme Middle East dust storm

Anthony J Parolari[1,6], Dan Li[2], Elie Bou-Zeid[3], Gabriel G Katul[4] and Shmuel Assouline[5]

[1] Department of Civil and Environmental Engineering, Duke University, Durham, NC 27708, USA
[2] Department of Earth and Environment, Boston University, Boston, MA 02215, USA
[3] Department of Civil and Environmental Engineering, Princeton University, Princeton, NJ 08544, USA
[4] Nicholas School of the Environment, Duke University, Durham, NC 27708, USA
[5] Department of Environmental Physics and Irrigation, Institute of Soil, Water and Environmental Sciences, A.R.O.-Volcani Center, Rishon LeTsion 7528809, Israel
[6] Present Address: Department of Civil, Construction, and Environmental Engineering, Marquette University, Milwaukee, WI 53233, USA.

E-mail: anthony.parolari@marquette.edu

OPEN ACCESS

RECEIVED
23 July 2016

REVISED
10 October 2016

ACCEPTED FOR PUBLICATION
21 October 2016

PUBLISHED
8 November 2016

Keywords: dust storms, wind erosion, drought, climate change

Supplementary material for this article is available online

Original content from this work may be used under the terms of the Creative Commons Attribution 3.0 licence.

Any further distribution of this work must maintain attribution to the author(s) and the title of the work, journal citation and DOI.

Abstract

The recent dust storm in the Middle East (Sepember 2015) was publicized in the media as a sign of an impending 'Dust Bowl.' Its severity, demonstrated by extreme aerosol optical depth in the atmosphere in the 99th percentile compared to historical data, was attributed to the ongoing regional conflict. However, surface meteorological and remote sensing data, as well as regional climate model simulations, support an alternative hypothesis: the historically unprecedented aridity played a more prominent role, as evidenced by unusual climatic and meteorological conditions prior to and during the storm. Remotely sensed normalized difference vegetation index demonstrates that vegetation cover was high in 2015 relative to the prior drought and conflict periods, suggesting that agricultural activity was not diminished during that year, thus negating the media narrative. Instead, meteorological simulations using the Weather Research and Forecasting (WRF) model show that the storm was associated with a cyclone and 'Shamal' winds, typical for dust storm generation in this region, that were immediately followed by an unusual wind reversal at low levels that spread dust west to the Mediterranean Coast. These unusual meteorological conditions were aided by a significant reduction in the critical shear stress due to extreme dry and hot conditions, thereby enhancing dust availability for erosion during this storm. Concluding, unusual aridity, combined with unique synoptic weather patterns, enhanced dust emission and westward long-range transport across the region, thus generating the extreme storm.

Introduction

Dust emission from the land surface plays a significant role in climate, biogeochemical cycling, and other earth system processes [1–3]; it can disrupt weather, public health, and economic activity. Sediment availability for emission is enhanced by aridity [4, 5], reduced vegetation cover [6, 7], and soil disturbance [8]; factors that may be linked to land use dynamics and human activity, including conflict. Dust emission is also enhanced by certain synoptic meteorological patterns, such as frontal and cyclonic systems known to generate dust storms in the Middle East [9–11]. It is becoming necessary to understand and attribute the relative influence of climate and human factors on dust emission.

In late August and early September 2015, an unusually severe dust storm occurred in the Middle East, the trajectory of which is illustrated in figure 1. Satellite images show that the dust storm emerged around 31 August, 2015 along the northeastern border between Syria and Iraq. The storm was delineated by a wall of dust and a cyclone clearly evident from the satellite imagery. Over the next two days, the cyclone moved southeast toward and across the Persian Gulf. Finally, the dust was spread westward, resulting in

© 2016 IOP Publishing Ltd

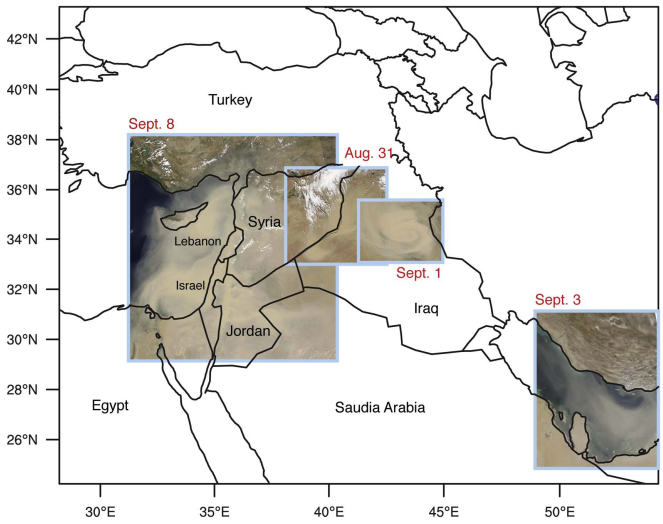

Figure 1. The trajectory of the September 2015 Middle East dust storm as observed by the Moderate Resolution Imaging Spectroradiometer (MODIS) satellite. The MODIS images track the dust storm from its inception on 31 August, 2015, near the northern Syria-Iraq border, to its peak on 8 September, over the Mediterranean coast. The images can be accessed at: worldview.earthdata.nasa.gov.

large portions of Syria, Lebanon, and the eastern Mediterranean Sea being obscured from the satellite view.

The Middle East is a notable hotspot dust source during the summer months and dust storms in this region are often associated with the Shamal (Arabic: شمال, 'north') winds and cyclones [2]. The greatest frequency and longest persistence of cyclones in this region is observed over Syria and Iraq [9]. Furthermore, the highest density of dust sources in the Middle East occurs in northern Iraq between the Tigris and Euphrates rivers and along the Syria–Iraq border [12], regions with extensive desert cover, low population densities, and sparse agriculture concentrated along river valleys. These previously characterized regions of frequent cyclogenesis and high density of dust sources coincide with the origination point of the storm (figure 1).

The September monthly average aerosol optical depth (AOD) in 2015 was elevated across the entire region, relative to the climatological average for the years 2000–2015 (figure 2(A)). Most strikingly, the Mediterranean coastal region of western Syria, Lebanon, and Israel exhibited September monthly average AOD three to four times the climatological average. Daily AOD data convey a similar story across the region with peak storm values on 8 September, 2015 in the 99th percentile of historical values (figure 2(B)). According to the historical data, daily AOD in the coastal region is typically less than that in the eastern, more arid part of the region; but was nearly twice as high during the peak of the storm (figure 2(B)). Therefore, this dust storm was characterized by high atmospheric aerosol concentrations that were unusually and particularly intensified over the Mediterranean coastal region.

With scores of people being hospitalized, several media reports popularized the dust storm as a symbol of the ongoing conflict in the Middle East (table 1). These reports blamed land cover change attributed to conflict, including agricultural land desertion, reduced irrigation, and increased military vehicle traffic over unpaved surfaces for the unusually severe storm. Because these reports lack empirical support, we developed and tested alternative hypotheses to further our understanding of what caused the unexpected nature of this storm. First, we analyzed vegetation cover data as an indicator of possible agricultural land abandonment stemming from conflict. Second, we conducted simulations using the Weather Research and Forecasting (WRF) model to characterize the synoptic circulation patterns during the storm. Finally, we investigated surface air temperature, humidity, and wind speed measurements to estimate the impact of aridity on soil cohesion and erodibility.

Methods

Methods include those for AOD, vegetation cover, WRF model simulations, and estimates of critical shear stress from surface temperature and relative humidity data. The impact of increased military traffic on dust emission could not be quantified due to a lack of data.

Aerosol optical depth

To evaluate the severity of the 2015 dust storm, Moderate Resolution Imaging Spectroradiometer (MODIS) AOD data were obtained. The AOD data are daily and monthly values computed by the Deep Blue algorithm over land. Relative AOD anomalies were computed for the September monthly average in 2015

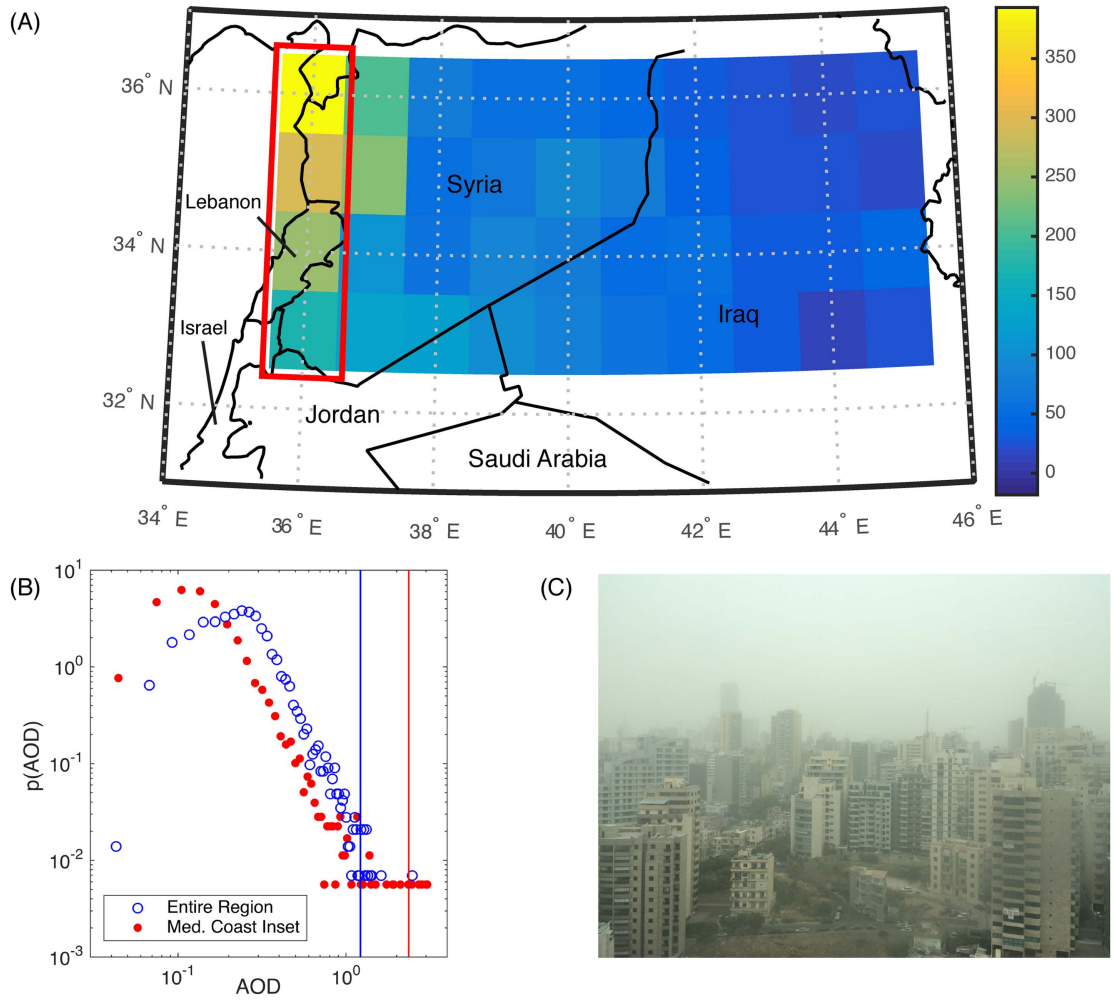

Figure 2. The September 2015 Middle East dust storm was characterized by an extreme concentration of suspended dust particles, as indicated by elevated aerosol optical depth (AOD) estimated from the Moderate Resolution Imaging Spectroradiometer (MODIS) satellite: (A) September monthly average AOD anomalies for 2015 relative to the 2000–2015 average, expressed as percent difference (see methods). (B) Probability distributions of daily AOD for the entire MODIS record (February 2000 through April 2016) for the entire region (blue dots) and for the red inset over the Mediterranean coast (red dots). The vertical blue and red lines denote the corresponding AOD values on 8 September, 2015, the peak AOD observed during the storm. (C) Photograph taken in Beirut on 8 September, 2015 by Elie Bou-Zeid.

Table 1. A list of news media reports describing popular explanations for the unusual severity of the September 2015 Middle East dust storm.

Publication	Date	Title
Motherboard	19 October, 2015	The Syrian War Is Causing a Dust Bowl in the Middle East, Researchers Suspect
Washington Post	7 October, 2015	Syria's war helped create an epic dust storm, scientists say
Haaretz	7 October, 2015	Syrian civil war contributed to unusual dust storm, say Israeli scientists
Washington Post	15 September, 2015	An epic Mideast sandstorm might have helped Syrian rebels
Jerusalem Post	11 September, 2015	Researchers stumped as dust storm persists in Israel for third day
Jerusalem Post	10 September, 2015	Israelis suffer through worst dust storm in 10 years
LBC-America	9 September, 2015	REPORT: Sandstorm hitting Lebanon currently ebbing
Al-Jazeera	9 September, 2015	Deadly sandstorm continues to blanket Middle East
The Times of Israel	8 September, 2015	Worst air pollution ever in Jerusalem as sandstorm engulfs Mideast
National Geographic	8 September, 2015	Explaining the Monster Dust Storm Sweeping the Middle East
BBC	8 September, 2015	Middle East dust storm puts dozens in hospital
Guardian News	8 September, 2015	Deadly sandstorm sweeps Lebanon and Syria
Al-Arabiyah	8 September, 2015	Unseasonal sandstorm hits Lebanon, Syria, Jordan and Israel
Naharnet	7 September, 2015	Scores hospitalized as 'Unprecedented' sandstorm engulfs several regions

relative to the period 2000–2015. AOD anomalies were computed as 2015 averages relative to historical averages and expressed as a percent difference, $\eta = \frac{A_{2015} - A_H}{A_H} \times 100$, where A_{2015} is the average AOD observed in September 2015 and A_H is the historical AOD average.

Vegetation cover

To estimate vegetation status in the region during the dust storm, MODIS Normalized Difference Vegetation Index (NDVI) was used. NDVI anomalies were computed as 2015 growing season (January through September) averages relative to historical averages, $\eta = \frac{N_{2015} - N_{\mathrm{H}}}{N_{\mathrm{H}}}$, where N_{2015} is the average NDVI observed January through September 2015 and N_{H} is the historical NDVI average. Historical averages were computed for non-drought (2001–2006) and drought (2007–2010) periods.

Ground meteorological data, soil matric potential, and wind erosion threshold

The physics of wind erosion are complex, as they involve atmospheric, soil, and land surface processes [13]. Wind erosion occurs when wind speed, u, exceeds a certain threshold value, u_t [14]. Several factors affect u_t, including field surface conditions, surface roughness, stability of the soil aggregates, size and shape of soil particles, clay content, vegetation cover, and near-surface soil moisture [15, 16]. Theoretical and empirical expressions have been proposed to relate u_t to soil surface moisture [15–23].

Studies describing the impact of mean wind on erosion usually use friction velocities, u_*, because they are directly related to the surface shear stress, τ, exerted on the soil surface ($\tau = \rho u_*^2$, ρ is the air density). Humidity affects the threshold u_{*t} and is known to vary on a global scale, as do dust emissions [5, 24]. This threshold evolves from the effect of inter-particle capillary forces (liquid bridge bonding) and hygroscopic forces (adsorbed layer bonding). The key macroscopic variable shaping these inter-particle bonding forces is the soil water matric potential, ψ [5, 16, 19, 25–27]. The Kelvin equation describes the dependence of ψ on relative humidity, RH, and surface temperature, $\psi = \left(\frac{RT}{V_{\mathrm{w}}}\right)\ln\left(\frac{RH}{100}\right)$ where R is the ideal gas constant (=8.314 J mol^{-1} K^{-1}), T is the surface temperature expressed in K, and V_{w} is the molar volume of water (=1.8 10^{-5} m^3 mol^{-1}). Under arid conditions, ψ is negative relative to atmospheric pressure. A model to relate relative humidity and temperature to the critical shear stress for particle motion, τ^*_t, is given as [5], $\tau_{*t} = f\left[\sigma g d + d^{-2}\frac{6a_i}{\pi a_l}\left(\beta_c d + \pi k d|\psi|\frac{\delta^{n+1}}{\delta_0^n}\right)\right]$, where $\delta = \sqrt[3]{\frac{A}{6\pi|\psi|}}$ and the parameters are defined in table 2. This is the model used to compute the critical shear stress shown in figure 5(D) using ground observations at the Israel meteorological service (IMS) station of Har Kenaan, Northern Israel.

Table 2. Parameter definitions and values for calculating critical shear stress from surface temperature and relative humidity data.

Parameter		Value	Units
Particle density	σ	1500	kg m^{-3}
Gravity constant	g	9.81	m s^{-2}
Ratio of moment arm lengths for interparticle and lift forces	a_i/a_l	1	
Particle diameter	d	100	μm
Electrostatic and van der Waals forces	$\beta_c d$	10^{-8}	N
Surface texture scale parameter	k	0.75×10^{-4}	
Monolayer film thickness	δ_0	0.3×10^{-9}	m
Layer scaling exponent	n	4.8	
Hamaker constant	A	-1.9×10^{-19}	J

WRF model simulations

An 11-day regional-scale simulation from 30 August to 10 September, 2015 was conducted using the Advanced Research Weather Research and Forecasting (WRF-ARW) Model over the Middle East. The simulation consists of two nested domains (d01 and d02), whose resolutions are 9 km and 3 km, respectively. Domain 1 (d01) covered a much larger area while domain 2 (d02) focused on the area where the dust storm was observed (figure S1). Domain 1 includes 300 (west–east) by 239 (north–south) grid cells in the horizontal directions and Domain 2 includes 451 (west–east) by 394 (north–south) grid cells. The top of the domain was set to 50 hPa and 35 vertical levels were used for both d01 and d02.

The WRF simulation was initialized using National Centers for Environmental Prediction FNL (Final) Operational Global Analysis data at 00 UTC on 30 August, 2015 and was forced by the same data set every six hours at the lateral boundaries of d01. One-way nesting was used (i.e., d02 was forced by d01 but did not provide any feedback to influence d01). The time steps were 30 s and 10 s for d01 and d02, respectively.

The physical parameterization schemes were chosen based on previous studies [28], including (1) the Dudhia scheme for shortwave radiation, (2) the Rapid Radiative Transfer Model scheme for longwave radiation, (3) the WRF Single-Moment 6-Class microphysics scheme, (4) the Yonsei University planetary boundary layer scheme, and (5) the Noah land surface model with the single-layer urban canopy model for cities. No cumulus parameterization was used due to the fact that the resolutions of the domains were both below 10 km. The radiation time step was chosen to be 10 min. The 30 s resolution MODIS land-cover data set was used, which includes 20 land-use categories. The resolutions of other static data (e.g., topography, soil type) were 5 min and 2 min for d01 and d02, respectively, to be consistent with the resolutions of the grids. The WRF simulated results agree favorably

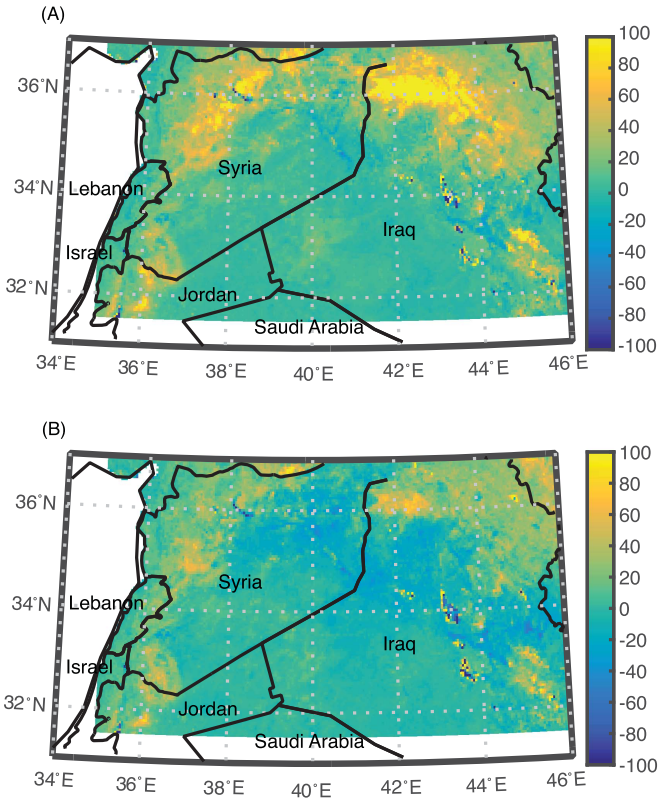

Figure 3. Normalized difference vegetation index (NDVI) anomalies comparing the 2015 growing season (January–September 2015) to (A) the multi-year average during a recent drought (January 2007–September 2010) and (B) the multi-year average for the five years prior to the drought (January 2001–September 2006). Anomalies are expressed as a percent difference.

with ground observations at Har Kenaan, Israel shown in figure S2 (supplementary material).

Results and discussion

Agriculture in northern Syria and Iraq was robust in 2015, despite a declining trend due to recent drought. It is estimated that nearly 1.5 million people migrated internally from rural agricultural areas to urban areas, initiated by a severe drought during 2007–2010 [29]. However, rainfall recovery following the most recent drought (2013 and 2014) resulted in greater than average vegetation density and wheat yields in 2015, both comparable to pre-drought conditions [30]. Across much of the region, vegetation cover in 2015 was nearly double the 2007–2010 average (figure 3(A)) and was also greater than the 2001–2007 pre-drought average (figure 3(B)) in many areas. Regions of vegetation decline were relatively sparse and concentrated near deserts. This finding indicates that land cover changes associated with the ongoing conflict were unlikely to be at the origin of increased erodibility of the soil surface and suggests meteorological conditions as the more probable driver for enhanced dust uplift and transport.

As mentioned earlier, dust storms in the Middle East are often associated with the Shamal winds and cyclones [11, 31]. To illustrate, figure 4 shows the low-level (700 hPa, figure 4(A)) and high-level (300 hPa, figure 4(C)) synoptic circulation patterns on 31 August, 2015 simulated using the WRF model (see the Material and Methods section). The Shamal was characterized by the northwesterly winds to the west of a low-pressure zone located slightly to the east of the northern Syria–Iraq border (figures 4(A) and (C)). However, the Shamal winds do not explain the extremely elevated dust concentrations over the Mediterranean coast on 7 and 8 September, as shown in figures 1 and 2. The WRF simulation results further reveal that on 6 September (figures 4(B) and (D)) the front moved to the north and persisted at 300 hPa, but not at 700 hPa. Interestingly, the low-level winds (figure 4(B)) showed a reversal as compared to the high-level winds that remained northwesterly (figure 4(D)). This surface wind reversal, subsequent to the cyclonic activity, likely both enhanced surface shear stress and transported previously suspended particles westward, thereby causing the extremely elevated dust concentrations along the Mediterranean coast. It is noted that westward dust transport in this region is not common [32].

In addition to the synoptic circulation patterns that favor dust storm genesis and development, surface air temperature and humidity measurements from the Har Kenaan meteorological station in Northern Israel show that the summer of 2015 was unusually dry and hot relative to the most recent 20 years

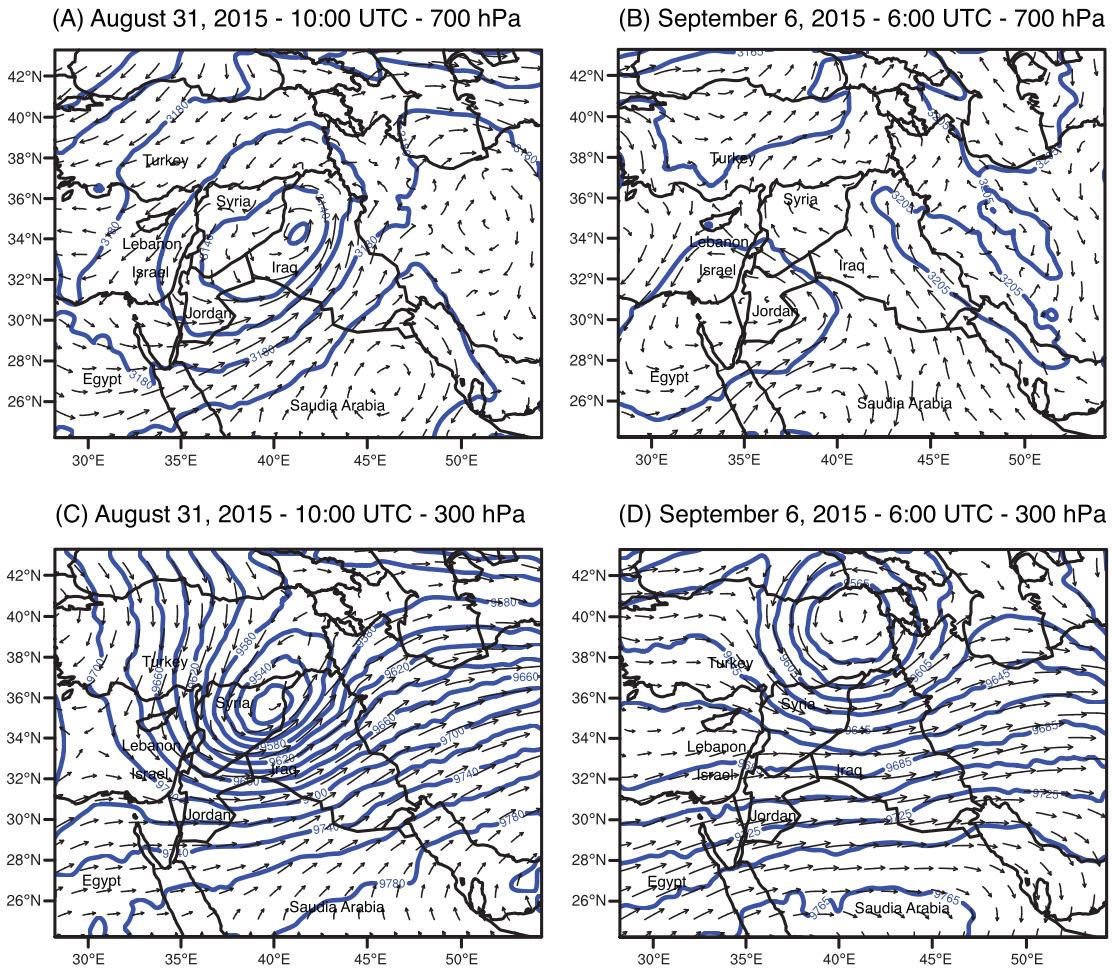

Figure 4. Synoptic conditions before and during the dust storm calculated using the WRF model: (A) 31 August, 2015 10:00 UTC lower-level (700 hPa) cyclonic circulation showing the low pressure area at the northern Syria/Iraq border and associated northwesterly Shamal winds. (B) 6 September, 2015 6:00 UTC (9:00 local time) lower-level (700 hPa) circulation showing easterly winds carrying emitted dust west into coastal Syria, Lebanon, and Israel. (C) and (D) upper-level (300 hPa) circulation showing the low pressure persistence throughout the storm between these two days. Blue contours show the geopotential height and gray arrows show the wind direction and magnitude.

(figures 5(B) and (C)). In fact, extreme high temperature and low humidity were more frequent during August and September 2015 than during the previous drought period 2007–2010. The soil matric potential, ψ, and related threshold shear stress required for wind erosion (see the Materials and Methods section), τ_{*t}, were lower during these dry and hot conditions (5), increasing the likelihood of dust emission. In the weeks preceding the dust storm, low humidity and high temperature extremes caused τ_{*t} to reach unusually low values. At times, τ_{*t} in August and September 2015 was approximately 75% relative to the average during 1994–2014 (figure 5(D)). Low τ_{*t} relative to average conditions implies easier and more likely dislodging of large dry dust particles into the atmosphere. Even if military vehicle traffic was a contributor to this dislodging, which remains a possible but not necessary factor in the genesis of this dust storm, it would have been aided by reduced particle cohesion due to extreme aridity. It has been suggested that long-term changes in atmospheric circulation over the region have increased aridity [29]. Therefore, such trends could affect the critical shear stress required for wind erosion, and may cause extreme dust storms to become more frequent in the region in the future.

Typically, Saharan dust particles range in diameter from $d_p = 0.1$–10 μm and the associated terminal velocity for this d_p range is 0.01–20 mm s^{-1} (3). Uplifting of dust particles to a minimum height of 1000 m by convective updrafts is reasonable. Given that the WRF predicted maximum boundary layer height exceeds 2 km, a minimum settling time of 14 h is plausible. The simulated easterly wind speed at 700 hPa on September 6 was approximately 30 km h^{-1}, giving a minimum travel distance ranging from 400 km (for $d_p = 10$ μm) to 800 000 km (for $d_p = 0.1$ μm) during such settling times. These travel distances are well within the domain area of interest and it can be surmised that particle size was not a limiting factor for long-range transport.

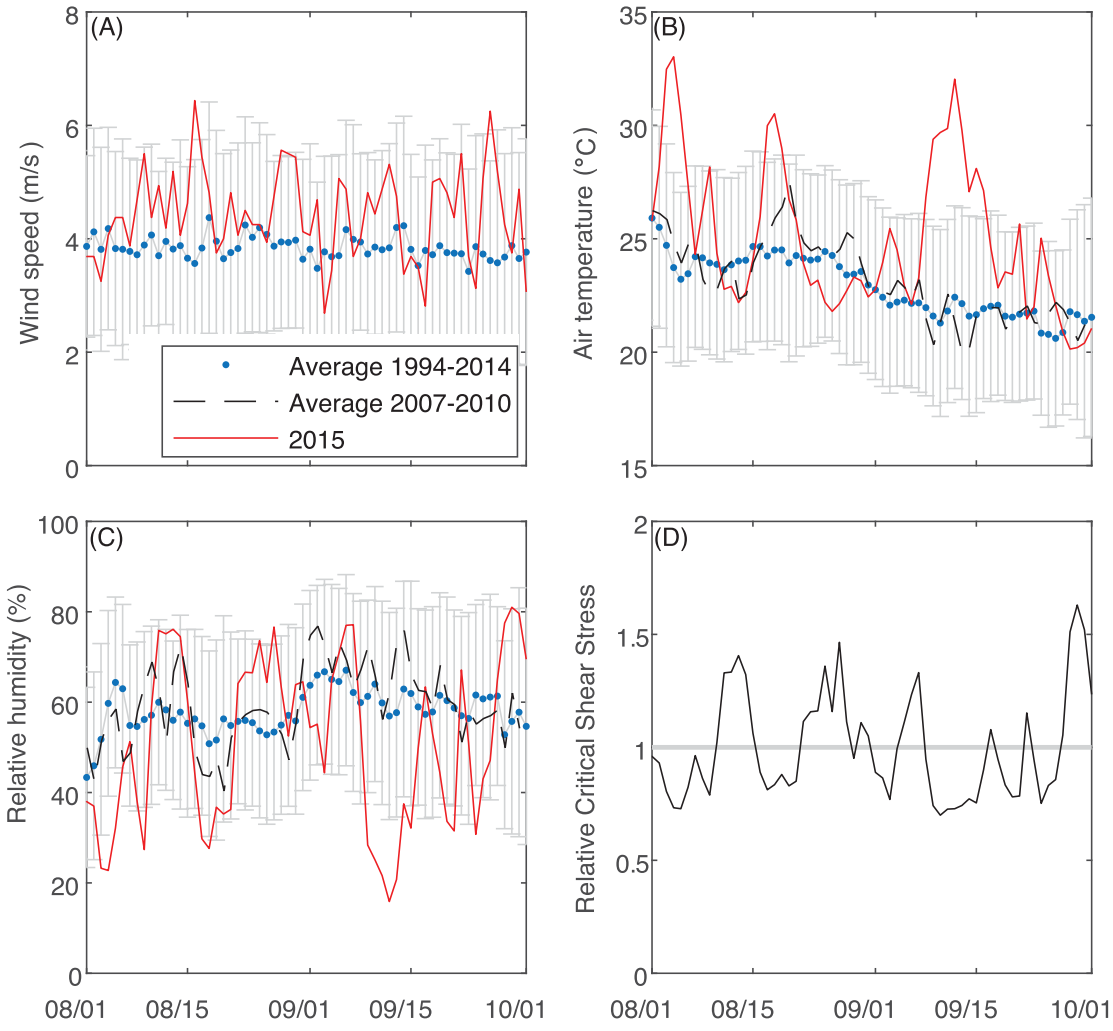

Figure 5. Aridity influence on soil erodibility: daily mean (A) wind speed, (B) air temperature, and (C) and relative humidity at Har Kenaan, Israel, during August and September 2015 (red lines) relative to historical values (blue dots indicate the 1994–2014 average, error bars indicate one standard deviation above and below the mean) and the previous drought period 2007–2010 (black dashed lines). Data are from the Israel Meteorological Service. (D) Estimated relative critical shear stress for dust emission relative to the historical average during 1994–2014 (see materials and methods section for details of critical shear stress calculation from surface temperature and humidity data).

Conclusion

Climate, land use, and conflict must be simultaneously acknowledged as elements in a complex human–environment relationship that has been playing out in the Middle East as far back as 4000 years ago, following the collapse of the Akkadian empire [33, 34]. Then and now, climate variability and control of scarce water resources have played a critical role in regional politics and conflicts [29] and their impacts on land use and land cover cannot be overlooked. Viewed from this perspective, it is understandable why the extreme 2015 dust storm was publicized as a sign of an impending 'Dust Bowl', and its severity attributed to the ongoing regional conflict. However, our analysis showed that aridity and synoptic meteorology played a prominent role in dust emission and transport for this episode. The storm occurred during a period of extreme aridity and was associated with a cyclone and 'Shamal' winds, typical for dust storm generation in this region. The Shamal was immediately followed by an unusual wind reversal at low levels that spread dust west to the Mediterranean Coast. This represents the key finding of this study and its importance is underscored by the reversibility of extreme dust events. Conflict-induced land cover change is reversible in the near term, potentially averting a persistent increase in dust storm frequency and severity; however, if such dust storms result from aridity and synoptic meteorology that could be significantly affected by climate change, then prolonged impacts in the Middle East may be unavoidable.

Acknowledgments

AJP and GGK acknowledge support from the US Department of Energy (DOE) through the Office of Biological and Environmental Research (BER) Terrestrial Carbon Processes (TCP) program (DE-

SC0006967, DE-SC0011461); the National Science Foundation (DGE-1068871, EAR-1344703) and the US Department of Agriculture through the Agriculture and Food Research Initiative (2011-67003-30222). The WRF simulations were performed on the supercomputing clusters of the National Center for Atmospheric Research through project P36861020. Ground data for the Har Kenaan station were provided by the Israel Meteorological Service data base.

References

[1] Kok J F, Parteli E J R, Michaels T I and Karam D B 2012 The physics of wind-blown sand and dust *Rep. Prog. Phys.* **75** 106901
[2] Choobari O A, Zawar-Reza P and Sturman A 2014 The global distribution of mineral dust and its impacts on the climate system: a review *Atmos. Res.* **138** 152–65
[3] Mahowald N *et al* 2014 The size distribution of desert dust aerosols and its impact on the Earth system *Aeolian Res.* **15** 53–71
[4] Ravi S and D'Odorico P 2005 A field-scale analysis of the dependence of wind erosion threshold velocity on air humidity *Geophys. Res. Lett.* **32** L21404
[5] McKenna-Neuman C and Sanderson S 2008 Humidity control of particle emissions in aeolian systems *J. Geophys. Res.* **113** F02S14
[6] Engelstaedter S, Kohfeld K E, Tegen I and Harrison S P 2003 Controls of dust emissions by vegetation and topographic depressions: an evaluation using dust storm frequency data *Geophys. Res. Lett.* **30** 1294
[7] Tegen I, Werner M, Harrison S P and Kohfeld K E 2004 Relative importance of climate and land use in determining present and future global soil dust emission *Geophys. Res. Lett.* **31** L05105
[8] Warren S D 2014 Role of biological soil crusts in desert hydrology and geomorphology: implications for military training operations *Military Geosciences in the Twenty-First Century* (*Geological Society of America Reviews in Engineering Geology*) ed R S Harmon *et al* 22nd edn, pp 177–86
[9] Trigo I F, Davies T D and Bigg G R 1999 Objective climatology of cyclones in the Mediterranean region *J. Clim.* **12** 1685–96
[10] Trigo I F, Bigg G R and Davies T D 2002 Climatology of cyclogenesis mechanisms in the mediterranean *Mon. Weather Rev.* **130** 549–69
[11] Rao P G, Hatwar H R, Al-Sulaiti M H and Al-Mulla A H 2003 Summer shamals over the Arabian Gulf *Weather* **58** 471–8
[12] Moridnejad A, Karimi N and Ariya P A 2015 A new inventory for middle east dust source points *Environ. Monit. Assess.* **187** 582
[13] Shao Y 2000 *Physics and Modeling of Wind Erosion* (Dordrecht: Kluwer)
[14] Ravi S, Zobeck T M, Over T M, Okin G S and D'Odorico P 2006 On the effect of moisture bonding forces in air-dry soils on threshold friction velocity of wind erosion *Sedimentology* **53** 597–609
[15] Chepil W S 1945 Dynamics of wind erosion: I. Nature of movement of soil by wind *Soil. Sci.* **60** 305–20
[16] Belly P-Y 1964 Sand Movement by Wind *Technical Memorandum No. 1* US Army Corps of Engineers (http://repository.tudelft.nl/islandora/object/uuid:f5051163-7a83-440d-9d02-92683a442549?collection=research)
[17] Bagnold R A 1941 *The Physics of Blown Sand and Desert* (Methuen, London)
[18] Gregory J M and Darwish M M 1990 Threshold friction velocity prediction considering water content *Winter meeting of the American Society of Agricultural Engineers (Chicago, IL)* Paper No. 902562
[19] McKenna-Neuman C and Nickling W G 1989 A theoretical and wind tunnel investigation of the effect of capillary water on the entrainment of sediment by wind *Can J. Soil. Sci.* **69** 79–96
[20] Fecan F, Marticorena B and Bergametti G 1998 Parametrization of the increase of the aeolian erosion threshold wind friction velocity due to soil moisture for arid and semi-arid areas *Ann. Geophys.* **17** 149–57
[21] Cornelis W M, Gabriels D and Hartmann R 2004 A parameterisation for the threshold shear velocity to initiate deflation of dry and wet sediment *Geomorphology* **59** 43–51
[22] Bisal F and Hsieh J 1966 Influence of soil moisture on erodibility of soil by wind *Soil Sci.* **102** 143–6
[23] Selah A and Fryrear D W 1995 Threshold wind velocities of wet soils as affected by wind blown sand *Soil Sci.* **160** 304–9
[24] Ravi S, D'Odorico P, Over T M and Zobeck T M 2004 On the effect of air humidity on soil susceptibility to wind erosion: the case of air-dry soils *Geophys. Res. Lett.* **31** L09501
[25] Haines W B 1925 Studies in the physical properties of soils: II. A note on the cohesion developed by capillary forces in an ideal soil *J. Agric. Sci.* **15** 529–35
[26] Fisher R A 1926 On the capillary forces in an ideal soil; correction to the formulae given by WB Haines *J. Agric. Sci.* **16** 492–505
[27] Shao Y and Lu H 2000 A simple expression for wind erosion threshold friction velocity *J. Geophys. Res.* **105** 22437
[28] Li D, Bou-Zeid E, Baeck M L, Jessup S and Smith J A 2013 Modeling land surface processes and heavy rainfall in urban environments: sensitivity to urban surface representations *J. Hydrometeorol.* **14** 1098–118
[29] Kelley C P, Mohtadi S, Cane M A, Seager R and Kushnir Y 2015 Climate change in the Fertile Crescent and implications of the recent Syrian drought *Proc. Natl Acad. Sci.* **112** 3241–6
[30] United States Department of Agriculture 2015 *SYRIA: 2015/2016 Wheat Production Up from Last Year due to Favorable Precipitation* (www.pecad.fas.usda.gov/highlights/2015/07/Syria/Index.htm)
[31] Hamidi M, Kavianpour M R and Shao Y 2013 Synoptic analysis of dust storms in the Middle East *Asia-Pacific J. Atmos Sci.* **49** 279–86
[32] Cao H, Amiraslani F, Liu J and Zhou N 2015 Identification of dust storm source areas in West Asia using multiple environmental datasets *Sci. Total Environ.* **502** 224–35
[33] Cullen H M *et al* 2000 Climate change and the collapse of the Akkadian empire: evidence from the deep sea *Geology* **28** 379–82
[34] Hsiang S M, Burke M and Miguel E 2013 Quantifying the influence of climate on human conflict *Science* **341** 1235367